

Supporting Information

Multiple charge-transfer excited states induced efficient and stable thermally activated delayed fluorescence

Teng Gao,^{ab} Jianjun Liu,^{*c} Guanhao Liu,^{ab} Yuanyuan Qin,^{ab} Shaogang Shen,^{ab} Honglei Gao,^{ab}
Xiangyu Dong,^{ab} Pengfei Wang,^{ab} Yong-Jin Pu,^{*c} and Ying Wang^{*ab}

^a. Key Laboratory of Photochemical Conversion and Optoelectronic Materials, and City U-CAS Joint Laboratory of Functional Materials and Device, Technical Institute of Physics and Chemistry, Chinese Academy of Sciences, Beijing 100190, China. E-mail: wangy@mail.ipc.ac.cn

^b. University of Chinese Academy of Sciences, Beijing, 100049, China.

^c. Center for Emergent Matter Science (CEMS), RIKEN, Wako, Saitama 351-0198, Japan. E-mail: jianjun.liu@riken.jp; yongjin.pu@riken.jp.

1. *Materials and methods*

All solvents and materials were used as received from commercial suppliers without further purification. All reactions were monitored by thin layer chromatographic analysis on a pre-coated silica gel plate, which was visualized by a UV lamp at 254 or 365 nm. Flash column chromatography was performed on glass column of silica gel (100–200 mesh) and solvent ratios were expressed in volume to volume. ¹H and ¹³C NMR spectra for structural characterization were recorded on NMR spectrometer (400 MHz for ¹H; 100 MHz for ¹³C). All NMR measurements were conducted in CDCl₃ at room temperature. The NMR spectra were recorded on VARIAN-GEMINI-300 and Bruker Avance II-400 spectrometer at room temperature and tetramethylsilane (TMS) as an internal reference. Mass spectra were recorded using a BIFLEXIII MALDI-TOF mass spectrometer in EI mode. Chemical shifts were reported as parts per million in scale using the solvent residual peak as internal standard for ¹H and ¹³C NMR. Coupling constants (*J*) were reported in Hertz (Hz). UV-vis spectra and fluorescence spectra were obtained with Hitachi U-3900 and F-4600 spectrophotometers, respectively. The phosphorescence spectra were measured in 2-MeTHF glass matrix at 77 K using a Hitachi F-4600 fluorescence spectrometer. The absolute fluorescence quantum yields of the solid films are measured with an integrating sphere. Cyclic voltammetry was performed using a CHI600A analyzer with a scan rate of 100 mV s⁻¹ at room temperature. The electrolytic cell was a conventional three-electrode cell with a glassy carbon working electrode, a platinum wire counter electrode, and a SCE (saturated calomel electrode) reference electrode. The measurement of oxidation potentials was performed in CH₂Cl₂ with

0.1 M of tetran-butylammonium hexafluorophosphate ($n\text{-Bu}_4\text{NPF}_6$) as a supporting electrolyte, and the reduction part was performed in THF with 0.1 M of $n\text{-Bu}_4\text{NPF}_6$ as a supporting electrolyte. The DSC measurements were carried out using a TA Instruments DSC 2910 thermal analyzer at a heating rate of $10\text{ }^\circ\text{C min}^{-1}$. The TGA measurements were performed on a TA Instruments TGA 2050 thermal analyzer. The diffraction experiments were carried out on a Rigaku Saturn 724 diffractometer equipped with a Mo-K α source at about 170 K. Crystal structures were solved with direct methods and refined with a full-matrix least-squares technique, using the SHELXS software package. Mercury (CSD software) was used for crystal structure visualization.

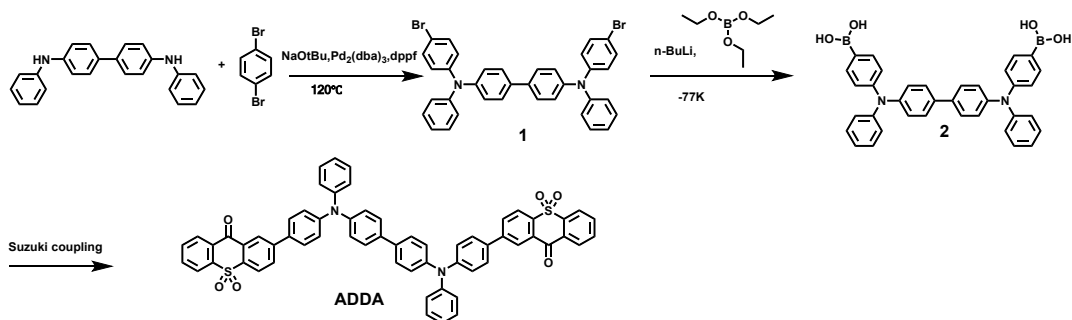
1.2 Synthesis. All solvents and materials were used as received from commercial suppliers without further purification. Synthetic routes of these compounds are shown in scheme S1 and S2.

Synthesis of *N,N'*-Diphenyl-*N,N'*-bis(4-bromophenyl)-biphenyl-4,4'-diamine(1): Tris(dibenzylideneacetone)-dipalladium ($\text{Pd}_2(\text{dba})_3$, 687 mg, 0.75 mmol) and diphenylphosphinoferrocene (dppf, 626 mg, 1.13 mmol) were dissolved in dry toluene under argon atmosphere. After 1,4-dibromobenzene (235 mg, 1 mol) was added, the reaction mixture was stirred for 10 min. To the mixture were added sodium-*tert*-butoxide (6010 mg, 62.5 mmol) and *N,N'*-diphenylbenzidine (8410 mg, 25 mmol). The reaction mixture was heated at $90\text{ }^\circ\text{C}$ overnight and deemed complete via thin layer chromatography (TLC) analysis. After being cooled to room temperature, the mixture was filtered through Celite and washed with toluene and water. The organic layer was extracted with toluene ($100\text{ mL} \times 3$) and dried over MgSO_4 . The solvent was evaporated on a rotary evaporator, and the dark brown mixture was purified by column chromatography on silica gel using methylene chloride/*n*-hexane (1:6) as eluent to give a white solid (Rf: 0.3). Yield: 11 g (68%). $^1\text{H NMR}$ (CDCl_3 , δ): 7.45 (d, 4H, $J = 8.53\text{ Hz}$), 7.34 (d, 4H, $J = 8.76\text{ Hz}$), 7.27 (t, 4H, $J = 8.20\text{ Hz}$), 7.12-7.03 (m, 10H), 6.99 (d, 4H, $J = 8.63\text{ Hz}$). $^{13}\text{C NMR}$ (CDCl_3 , δ): 147.23, 146.87, 146.36, 135.13, 132.22, 129.44, 127.49, 125.32, 124.56, 124.32, 123.41, 114.99. EIMS m/z (%): calcd for $\text{C}_{36}\text{H}_{26}\text{Br}_2\text{N}_2$, 646.43; found: 646.04.

Synthesis of ((1,1'-biphenyl)-4,4'-diylbis(phenylazanediy))bis(4,1-phenylene)diboronic acid(2): Dried THF (100 ml) and *N,N'*-Diphenyl-*N,N'*-bis(4-bromophenyl)-biphenyl-4,4'-diamine (646 mg, 1 mmol) were mixed in a 250 ml three-necked flask equipped with a condenser and mechanical stirrer under nitrogen. $n\text{-BuLi}$ (1 ml, 2.5 M in hexane) was added dropwise to the reaction mixture which was cooled to $-78\text{ }^\circ\text{C}$ over a period of 30 min. The reaction mixture was stirred at $-78\text{ }^\circ\text{C}$ for 2 h. After lithiation, triethyl borate (0.42 ml, 2.5 mmol) was rapidly added to the reaction mixture which was cooled to $-78\text{ }^\circ\text{C}$. The solution was stirred at room temperature for another 12 h. The reaction mixture was poured into a mixture of ice and water, acidified with 2 N HCl and extracted with dichloromethane successively. Then the organic phase was washed three times with water, and dried over MgSO_4 . The crude product was obtained as white powder by recrystallization from ethanol and diethyl ether. And

the crude product was used in the subsequent reaction without further purification.

Synthesis of 2,2'-((1,1'-biphenyl)-4,4'-diylbis(phenylazanediyl))bis(4,1-phenylene))bis(9H-thioxanthen-9-one 10,10-dioxide)(ADDA): 2-bromo-9H-thioxanthen-9-one 10,10-dioxide (802 g, 2.5 mmol), tetrakis (triphenylphosphine) palladium(0) (83 mg, 0.072 mmol), 2 M K₂CO₃ (20 ml) and toluene (40 ml) were added to a 250 ml three-necked flask under nitrogen. The prepared ((1,1'-biphenyl)-4,4'-diylbis(phenylazanediyl))bis(4,1-phenylene)diboronic acid (576 mg, 1 mmol) was added to the solution and heated to 98 °C for 6 h. After cooling to room temperature, the reaction mixture was diluted with dichloromethane and the organic phase was washed with water. After drying over MgSO₄, the solvent was removed. The resulting crude product was passed through a flash column chromatograph to remove impurities and recrystallized from ethanol to obtain a yellow solid product. The yield of product was 73%. ¹H NMR (CDCl₃, δ): 8.53 (s, 1H), 8.37 (d, J = 7.7 Hz, 1H), 8.21 (dd, J = 7.8, 2.9 Hz, 2H), 8.05 (d, J = 8.2 Hz, 1H), 7.89 (t, J = 7.5 Hz, 1H), 7.80 (t, J = 7.6 Hz, 1H), 7.56 (dd, J = 19.4, 8.5 Hz, 4H), 7.34 (t, J = 7.7 Hz, 2H), 7.28 – 7.19 (m, 6H), 7.13 (t, J = 7.2 Hz, 1H). ¹³C NMR (C₂Cl₄D₂, δ): 178.81, 148.90, 146.97, 146.20, 145.97, 140.90, 138.06, 135.33, 134.99, 133.57, 132.20, 131.26, 130.95, 129.74, 129.41, 128.23, 127.64, 126.81, 125.35, 125.26, 124.38, 124.11, 123.58, 123.05. EIMS m/z (%): calcd for C₆₂H₄₀N₂O₆S₂, 973.13; found: 972.24.

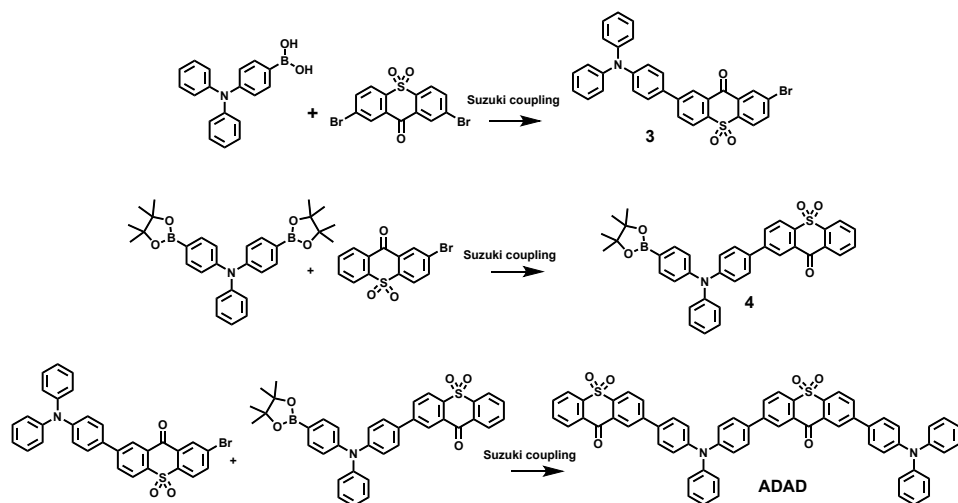


Scheme S1. Synthetic Routes of ADDA.

Synthesis of 2-bromo-7-(4-(diphenylamino)phenyl)-9H-thioxanthen-9-one 10,10-dioxide(3): 2,7-dibromo-9H-thioxanthen-9-one 10,10-dioxide (401 mg, 1 mmol), tetrakis (triphenylphosphine) palladium(0) (83 mg, 0.072 mmol), 2 M K₂CO₃ (20 ml) and toluene (40 ml) were added to a 250 ml three-necked flask under nitrogen. The prepared (4-(diphenylamino)phenyl)boronic acid (289 mg, 1 mmol) was added to the solution and heated to 98 °C for 6 h. After cooling to room temperature, the reaction mixture was diluted with dichloromethane and the organic phase was washed with water. After drying over MgSO₄, the solvent was removed. The resulting crude product was passed through a flash column chromatograph to remove impurities and recrystallized from ethanol to obtain a light yellow solid product. The yield of product was 59%. ¹H NMR (CDCl₃, δ): 8.49 (dd, J = 5.2, 1.7 Hz, 2H), 8.19 (d, J = 8.2 Hz, 1H), 8.09–7.97 (m, 3H), 7.55 (d, J = 8.7 Hz, 2H), 7.31 (t, J = 7.9 Hz, 4H), 7.21–7.06 (m, 8H). EIMS m/z (%): calcd for C₃₁H₂₀BrNO₃S, 566.47; found: 565.03, 567.03.

Synthesis of 2-(4-(phenyl(4-(4,4,5,5-tetramethyl-1,3,2-dioxaborolan-2-yl)phenyl)amino)phenyl)-9H-thioxanthen-9-one 10,10-dioxide(4): 2-bromo-9H-thioxanthen-9-one 10,10-dioxide (321 mg, 1 mmol), tetrakis (triphenylphosphine) palladium(0) (83 mg, 0.072 mmol), 2 M K₂CO₃ (20 ml) and toluene (40 ml) were added to a 250 ml three-necked flask under nitrogen. The prepared N-phenyl-4-(4,4,5,5-tetramethyl-1,3,2-dioxaborolan-2-yl)-N-(4-(4,4,5,5-tetramethyl-1,3,2-dioxaborolan-2-yl) phenyl) aniline (497 mg, 1 mmol) was added to the solution and heated to 96 °C for 6 h. After cooling to room temperature, the reaction mixture was diluted with dichloromethane and the organic phase was washed with water. After drying over MgSO₄, the solvent was removed. The resulting crude product was passed through a flash column chromatograph to remove impurities and recrystallized from ethanol to obtain a light yellow solid product. The yield of product was 62%. ¹H NMR (CDCl₃, δ): 8.52 (s, 1H), 8.37 (d, J = 7.4 Hz, 1H), 8.21 (d, J = 7.6 Hz, 2H), 8.04 (d, J = 8.1 Hz, 1H), 7.89 (t, J = 7.1 Hz, 1H), 7.80 (t, J = 7.5 Hz, 1H), 7.73 (d, J = 7.6 Hz, 2H), 7.56 (d, J = 7.9 Hz, 2H), 7.35–7.29 (m, 3H), 7.22–7.09 (m, 7H), 1.35 (s, 12H). EIMS m/z (%): calcd for C₃₇H₃₂BNO₅S, 613.54; found: 613.21.

Synthesis of 2-(4-(4-(10,10-dioxido-9-oxo-9H-thioxanthen-2-yl)phenyl)(phenyl)amino)phenyl)-7-(4-(diphenylamino)phenyl)-9H-thioxanthen-9-one 10,10-dioxide(ADAD): 2-bromo-7-(4-(diphenylamino)phenyl)-9H-thioxanthen-9-one 10,10-dioxide (565 mg, 1 mmol), tetrakis (triphenylphosphine) palladium(0) (83 mg, 0.072 mmol), 2 M K₂CO₃ (20 ml) and toluene (40 ml) were added to a 250 ml three-necked flask under nitrogen. The prepared 2-(4-(phenyl(4-(4,4,5,5-tetramethyl-1,3,2-dioxaborolan-2-yl)phenyl)amino)phenyl)-9H-thioxanthen-9-one 10,10-dioxide (731 mg, 1.2 mol) was added to the solution and heated to 96 °C for 6 h. After cooling to room temperature, the reaction mixture was diluted with dichloromethane and the organic phase was washed with water. After drying over MgSO₄, the solvent was removed. The resulting crude product was passed through a flash column chromatograph to remove impurities and recrystallized from ethanol to obtain a light yellow solid product. The yield of product was 57%. ¹H NMR (CDCl₃, δ): 8.55 (d, J = 6.6 Hz, 3H), 8.38 (d, J = 7.7 Hz, 1H), 8.23 (td, J = 7.8, 3.7 Hz, 4H), 8.06 (t, J = 7.6 Hz, 3H), 7.90 (t, J = 7.6 Hz, 1H), 7.81 (t, J = 7.6 Hz, 1H), 7.65 – 7.54 (m, 6H), 7.40 – 7.27 (m, 8H), 7.26 – 7.13 (m, 11H), 7.10 (t, J = 7.3 Hz, 2H). ¹³C NMR (CD₂Cl₂, δ): 178.93, 148.77, 148.74, 147.61, 147.14, 141.59, 135.17, 133.64, 132.55, 132.41, 131.58, 131.23, 130.10, 129.86, 129.50, 128.66, 128.42, 127.05, 126.91, 126.17, 126.14, 125.52, 124.92, 124.52, 124.46, 124.43, 124.35, 124.28, 124.16, 123.71, 123.09. EIMS m/z (%): calcd for C₆₂H₄₀N₂O₆S₂, 973.13; found: 972.24.



Scheme S2. Synthetic Routes of ADAD.

1.3 Theoretical calculations.

The molecular geometries of the isomers were optimized by density functional theory (DFT). Based on the optimized geometries, time-dependent DFT (TDDFT) was then used to calculate the excitation energies and transition characters of the lowest singlet (S_1) and triplet (T_1) excited states. although the B3LYP functional is inapplicable to describe the electronic properties in the gas phase, it can reasonably describe the solid-state properties, including both molecular levels and the lowest excited states; moreover, the B3LYP-calculated ΔE_{ST} values are almost unchanged by different dielectric constants. Therefore, all these calculations were carried out with the B3LYP functional and the 6-31G** basis set in the gas phase, as implemented in the Gaussian 09 package.

1.4 Device fabrication.

Before device fabrication, the ITO glass substrates were sequentially cleaned with detergents, de-ionized water, acetone, ethanol, dried at 75 °C, and treated with oxygen plasma for 10 min. After that, the clean substrates were transferred into a vacuum deposition system with a pressure below 5×10^{-4} Pa for organic and metal deposition. The devices were fabricated by evaporating organic materials onto the substrate at a rate of 1-2 \AA s^{-1} while LiF at a rate of 0.05 \AA s^{-1} and Al metal through a rate of 2 \AA s^{-1} . Then capped with EL luminescence spectra and CIE color coordinates were measured with a Spectrascan PR650 photometer and the current-voltage characteristics were measured with a computer-controlled Keithley 2400 Source Meter and CS-200 under ambient atmosphere.

2. Supplementary tables and figures

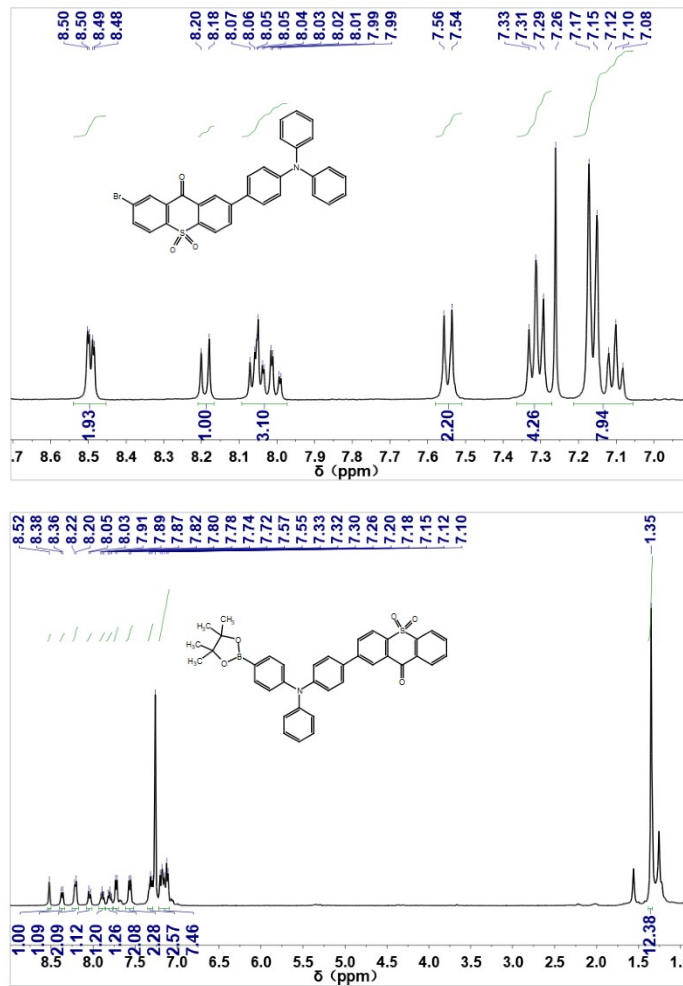
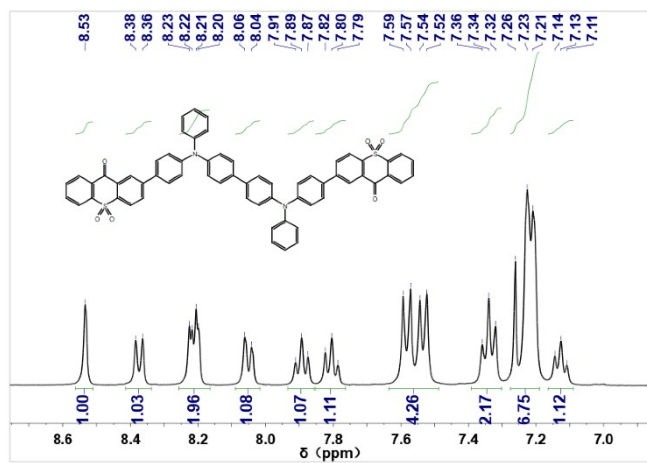


Fig S1. ¹H NMR spectrum of intermediate products.



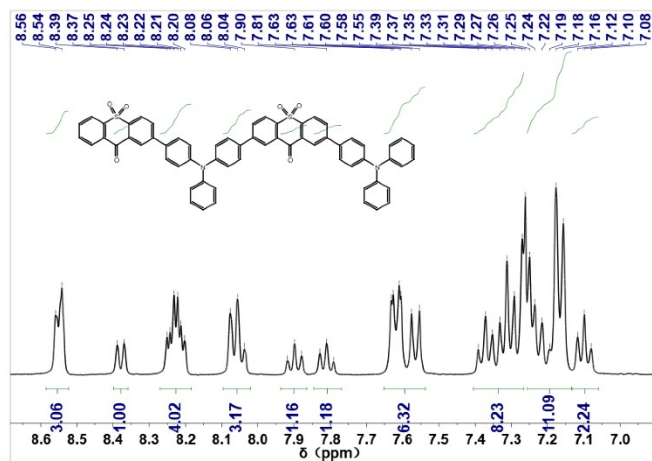


Fig S2. ^1H NMR spectrum of ADAD and ADDA.

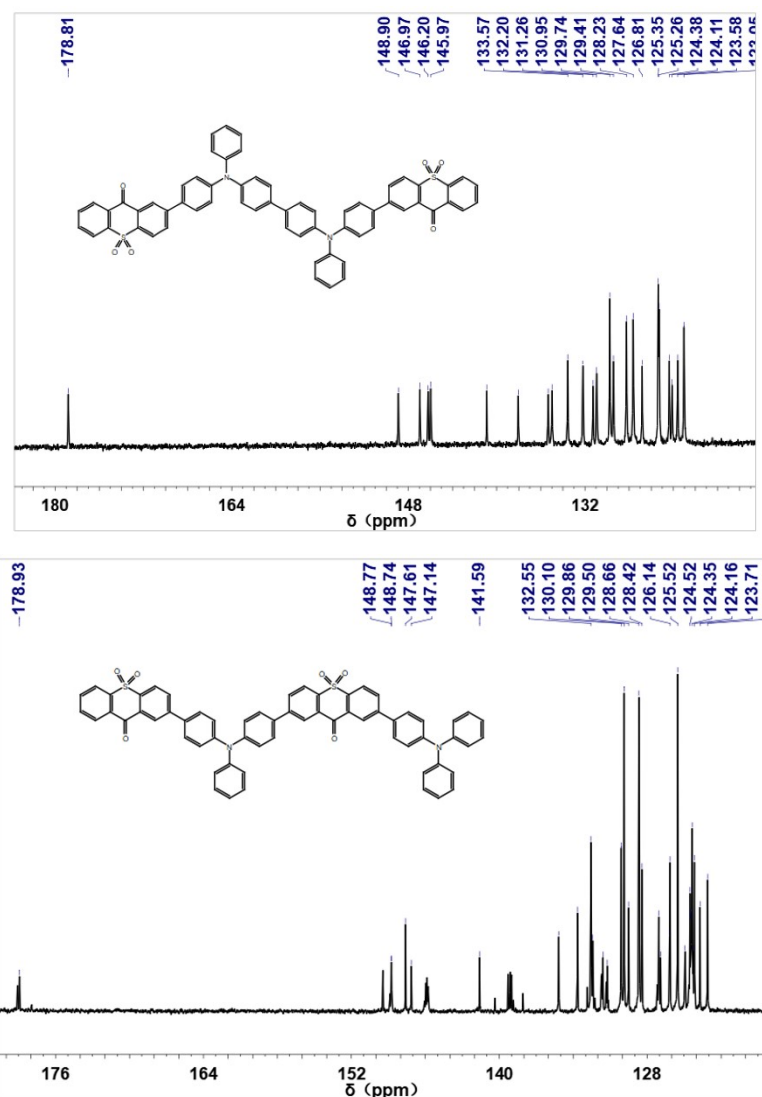


Fig S3. ^{13}C NMR spectrum of ADAD and ADDA.

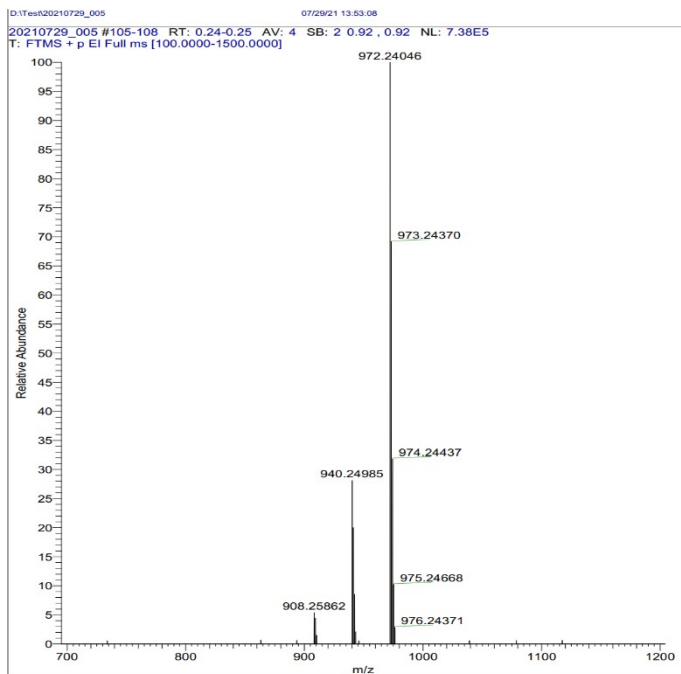


Fig S4. HRMS EI+ spectrum of ADAD.

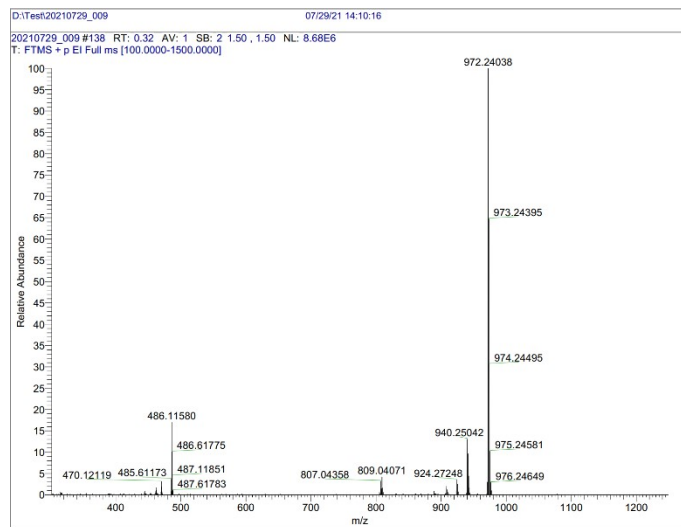


Fig S5. HRMS EI+ spectrum of ADDA.

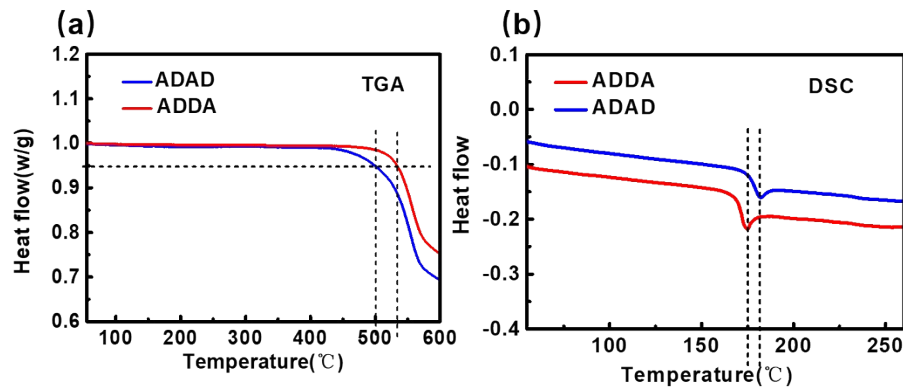


Fig S6. Thermodynamic properties of compounds. a) TGA curves of ADAD and ADDA and b) DSC curves of ADAD and ADDA.

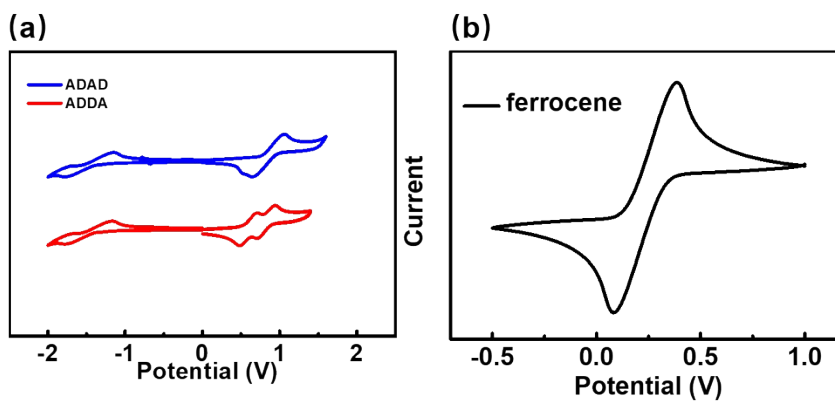


Fig S7. Cyclic voltammetry curves of a) ADAD, ADDA and b) reference ferrocene.

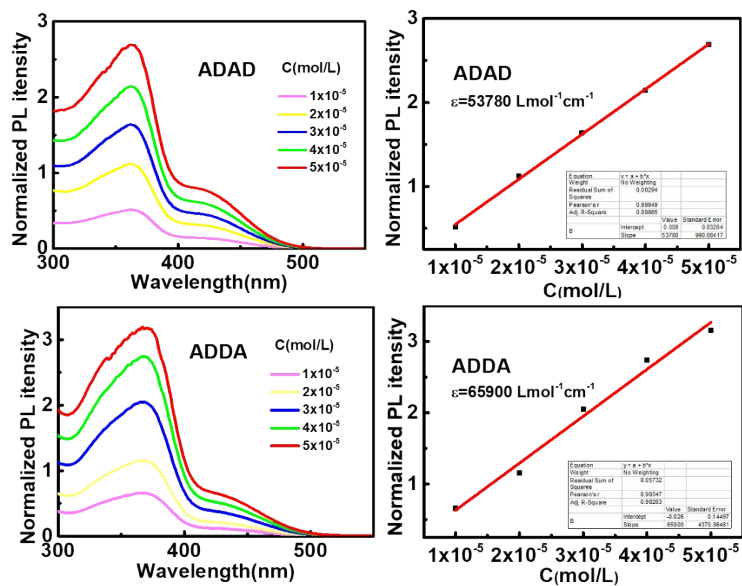


Fig S8. Concentration dependence of the absorbance of ADAD and ADDA in toluene.

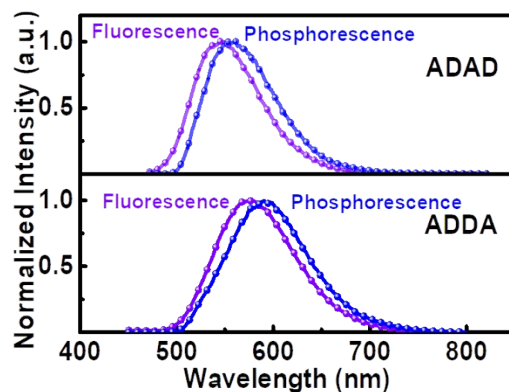


Fig S9. Normalized fluorescence and phosphorescence spectra of ADAD and ADDA in 2-MeTHF at 77 K, excited at 420 nm

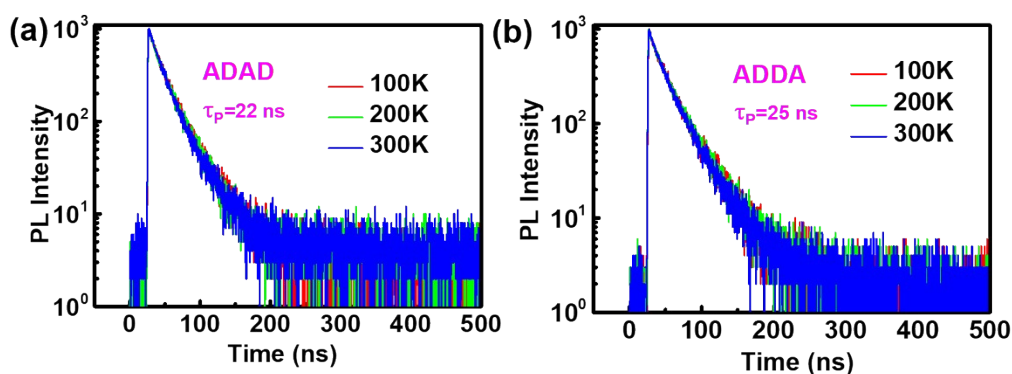


Fig S10. Temperature-dependence of the transient PL spectra of doped films in time range of 100 ns under vacuum. (a)ADAD and (b)ADDA. (All films were doped in 35DCzPPY with the ratio of 4%. Excitation source: 405 nm EPL Laser)

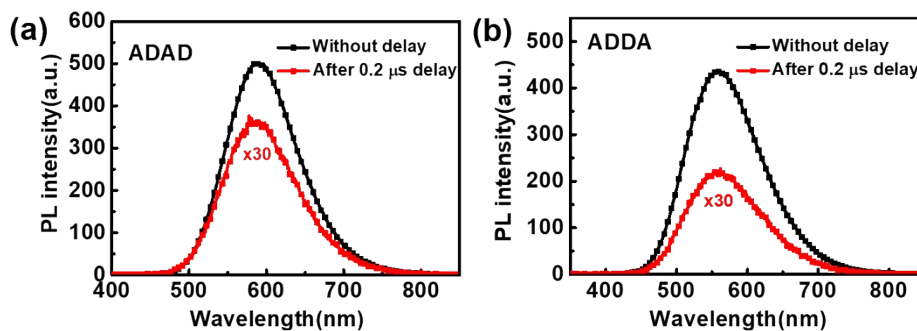


Fig S11. a) PL spectra of 4 wt% ADAD: 35DCzPPy film at 300 K without delay and with a delay of 0.2 μ s; b) PL spectra of 4 wt% ADDA: 35DCzPPy film at 300 K without delay and with a delay of 0.2 μ s.

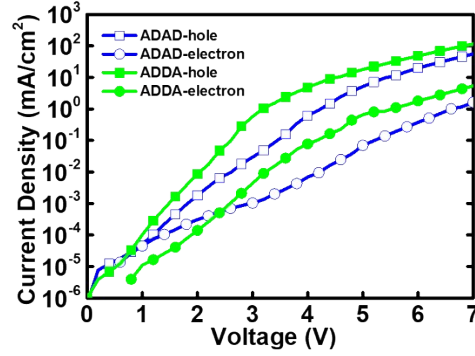


Fig S12. The hole-only and electron-only devices based on ADAD and ADDA.

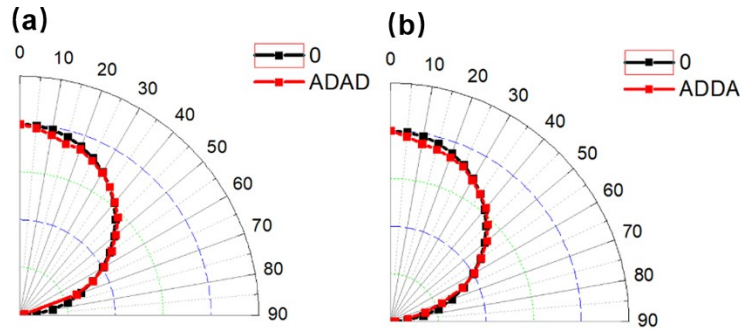


Fig S13. Angular dependent EL emission pattern of a) ADAD and b) ADDA TADF devices. The black line is Lambertian distribution.

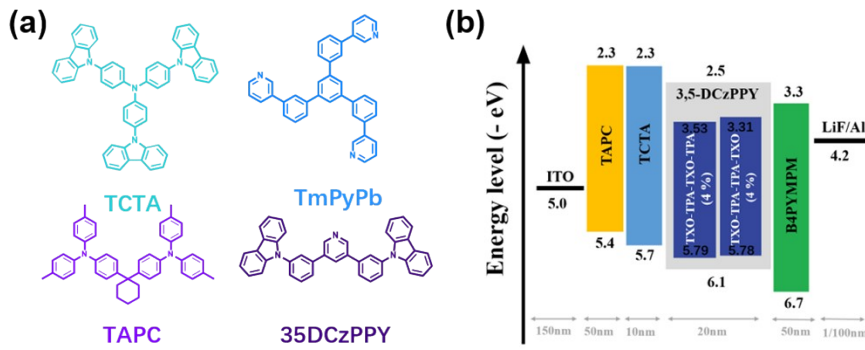


Fig S14. The energy levels and molecular structures for the device construction.

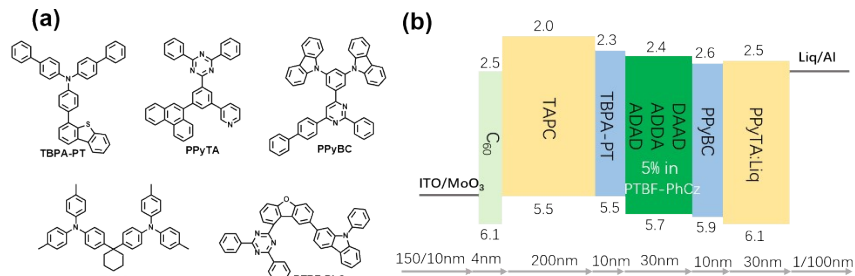


Fig S15. Molecular structures of organic materials used for fabricating OLEDs and energy level diagram of these OLEDs: (a) molecular structures; (b) energy level diagrams of these OLEDs.

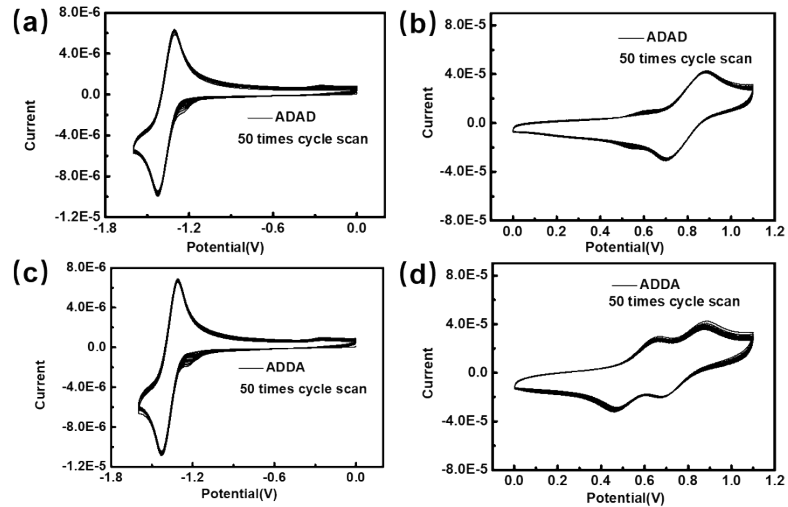


Fig S16. The multiple Cyclic voltammetry curves of ADAD and ADDA.

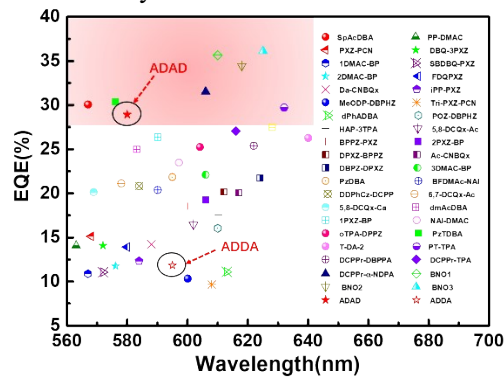


Fig S17. Summary of wavelength versus EQE plot of orange-red TADF materials reported in the literature.

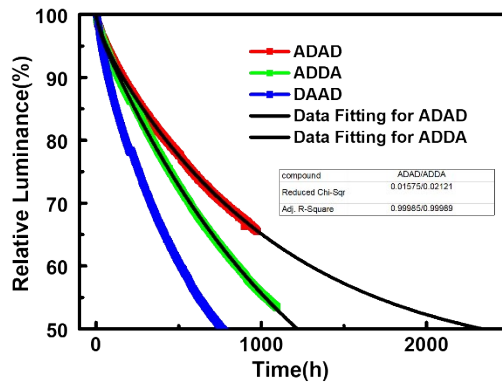


Fig S18. Luminance variation curves over operational time of doped device based on ADAD, ADDA and DAAD at an initial luminance of 1000 cd m^{-2} .

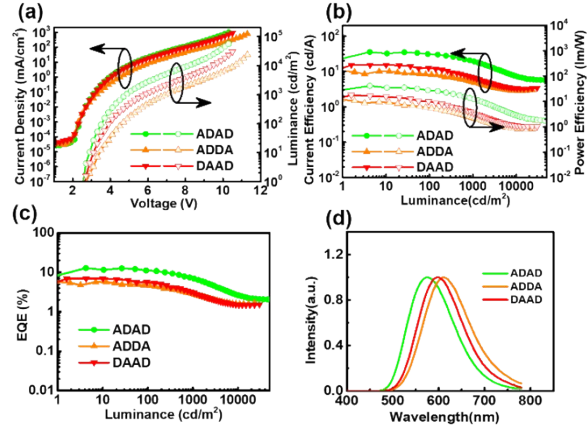


Fig S19. (a)Current density–voltage–luminescence (J–V–L) characteristics. (b)Power efficiency versus luminance characteristics. (c)External quantum efficiency versus luminance characteristics for OLED device. (d)The EL spectra of the devices based on ADDA, ADAD and DAAD.

Table S1. The spin-orbit coupling parameter of ADAD and ADDA; Overlapping integration of "particles" and "holes" in the S_1 - S_4 and T_1 - T_4 excited states of ADAD and ADDA.

ADAD/ADDA	SOC (cm^{-1})	ADAD/ADDA	$\langle\Psi_H \Psi_L\rangle$
$\langle S_1 H_{\text{SO}} T_1\rangle$	0.088/0.077	S_1	0.23/0.19
$\langle S_1 H_{\text{SO}} T_2\rangle$	0.089/0.007	S_2	0.22/0.19
$\langle S_1 H_{\text{SO}} T_3\rangle$	0.440/-	S_3	0.04/0.15
$\langle S_1 H_{\text{SO}} T_4\rangle$	0.009/-	T_1	0.38/0.29
$\langle S_2 H_{\text{SO}} T_1\rangle$	0.067/0.047	T_2	0.39/0.27
$\langle S_2 H_{\text{SO}} T_2\rangle$	0.139/0.101	T_3	0.40/0.22
$\langle S_2 H_{\text{SO}} T_3\rangle$	0.062/-		
$\langle S_2 H_{\text{SO}} T_4\rangle$	0.183/-		
$\langle S_3 H_{\text{SO}} T_1\rangle$	0.030/-		
$\langle S_3 H_{\text{SO}} T_2\rangle$	0.179/-		
$\langle S_3 H_{\text{SO}} T_3\rangle$	0.037/-		
$\langle S_3 H_{\text{SO}} T_4\rangle$	0.020/-		
$\langle S_4 H_{\text{SO}} T_1\rangle$	0.443/-		
$\langle S_4 H_{\text{SO}} T_2\rangle$	0.041/-		
$\langle S_4 H_{\text{SO}} T_3\rangle$	0.110/-		
$\langle S_4 H_{\text{SO}} T_4\rangle$	0.026/-		

Table S2. The summary of computing transient characterization in doped films.

	Φ_{Total} (%)	Φ_{prompt} (%)	Φ_{TADF} (%)	Φ_{T} (%)	K_{S} (s^{-1})	K_{ISC} (s^{-1})	k^{SR} (s^{-1})
ADAD	92.4	0.13	92.26	99.85	4.50×10^7	4.50×10^7	6.12×10^4
ADDA	53.3	0.78	52.52	98.52	3.92×10^7	3.86×10^7	3.07×10^5

Table S3. The OLED performance of the lifetime-tested OLEDs based on ADAD, ADDA and DAAD.

	V_{on}/V	$L_{V_{max}}/cd\ m^{-2}$	EQE/%	$CE/cd\ A^{-1}$	$PE/lm\ W^{-1}$
ADAD	2.7	55942	12.87	35.55	41.36
ADDA	2.9	23388	5.67	9.67	10.48
DAAD	2.7	29974	6.98	15.27	17.77